Acta Geotechnica (2015) 10:305–318
DOI 10.1007/s11440-014-0362-8

REVIEW

Embankment overtopping protection systems

Hubert Chanson

Received: 27 March 2013 / Accepted: 27 August 2014 / Published online: 23 December 2014

Abstract For the last decades, the design floods of numerous embankment reservoirs were re-evaluated, and the revised spillway outflows are typically larger than those used in the original designs. As a result, a number of overtopping protection systems were developed for embankments and earthfill dams, with applications encompassing river dykes, coastal barriers for storm surge and tsunami protections. Several design techniques were developed for embankments and earthfill dams. These include concrete overtopping protection systems, timber cribs, sheet-piles, riprap and gabions, reinforced earth, minimum energy loss weirs, embankment overflow stepped spillways and the precast concrete block protection systems. Various designs are reviewed herein and discussed based upon prototype experiences. This review highlights that a safe operation of embankment overflow protection systems relies upon a sound design and a good quality of construction, suitable flow conditions, together with regular maintenance.

Keywords Design techniques · Earthfill structures · Embankment · Overflow protection systems · Prototype experience · Spillways

Abbreviations
MEL Minimum energy loss
RCC Roller compacter concrete

1 Introduction

Worldwide, the design floods of numerous reservoirs were re-evaluated, and the revised spillway outflows are typically larger than those used in the original design. The occurrence of these larger floods could result in dam overtopping with catastrophic consequences when an insufficient storage or spillway capacity is available. A number of overtopping protection systems were developed for embankments and earthfill dams. These include concrete overtopping protection systems, timber cribs, sheet-piles, riprap and gabions, reinforced earth, minimum energy loss (MEL) weirs, embankment overflow stepped spillways and the precast concrete block protection systems developed by the Russian engineers [4, 14]. Herein, an embankment is considered as an earthfill structure designed to hold water. This definition encompasses river dykes, coastal barriers for storm surge and tsunami protections, as well as natural lakes and landslide dams (Figs. 1, 2). Figure 1 presents some typical embankment dam structures, and Fig. 2 shows some embankments for coastal protection.

All these structures are potentially erodible when overtopped, unless an overtopping protection system is designed. During the nineteenth to twenty-first centuries, numerous embankment structures failed worldwide (Fig. 3). With embankment dams, the two most common causes of failures were dam overtopping and cracking in the earthfill. The former issue is linked with inadequate spillway capacity, while the latter is the result of a

Electronic supplementary material The online version of this article (doi:10.1007/s11440-014-0362-8) contains supplementary material, which is available to authorized users.

H. Chanson (✉)
School of Civil Engineering, The University of Queensland, Brisbane, QLD 4072, Australia
e-mail: h.chanson@uq.edu.au
URL: http://www.uq.edu.au/~e2hchans/

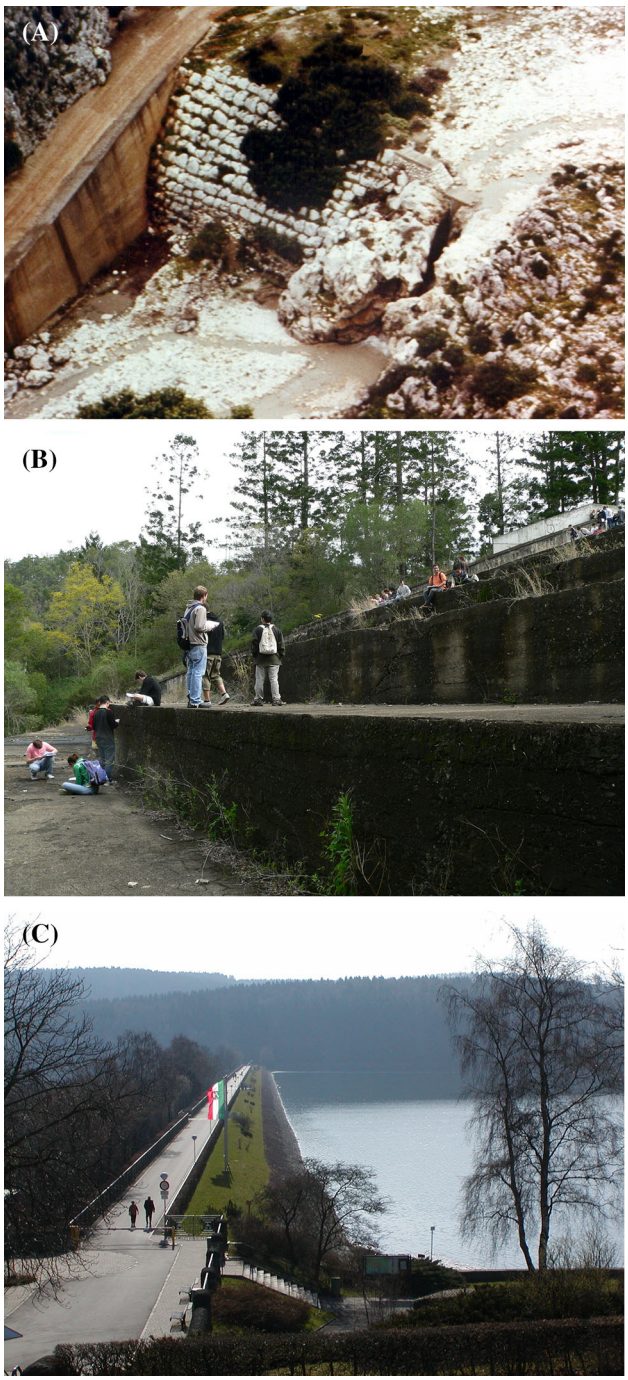

Fig. 1 Examples of embankment dam structures. **a** Embankment dam with overtopping stepped spillway: stepped weir in Akarnania (Greece) (Courtesy of Professor Knauss)—completion: BC 1,300, $H = 10.5$ m, $L = 25$ m, **b** concrete stepped spillway of Gold Creek dam (Australia) with the embankment dam in the background—completion: 1885, $H = 26$ m, $L = 187$ m—the concrete spillway was built over the right abutment, **c** embankment dam: Sorpe dam (Germany) on 31 March 2004 viewed from left bank—completion: 1935, $H = 69$ m, $L = 700$ m

Fig. 2 Examples of river and coastal embankments. **a** Coastal barrier in Netherlands: Zeidersee enclosure dam (Courtesy of Ronald De Heer), **b** tidal bore of the Qiantang River (China) overtopping a river dyke on 31 August 2011, **c** physical model of a coastal barrier during a tsunami—physical test with tsunami wave model propagating from *right to left* and impacting the embankment

combination of poor understanding of geotechnical concepts, inappropriate construction standards and internal failure (Fig. 3a). In recent years, a number of large floods caused dam overtopping because of the insufficient storage and spillway capacity of existing reservoirs. Figure 3b–d illustrates some examples of catastrophic failures. In each case, the spillway capacity became insufficient during a major hydrological event. A related form of embankment dams is the "natural dam" created by landslides and rockslides. For example, during the May 2008 earthquake in the Sichuan Basin (China), several lakes were formed, and some were artificially breached because they were natural hazards [52].

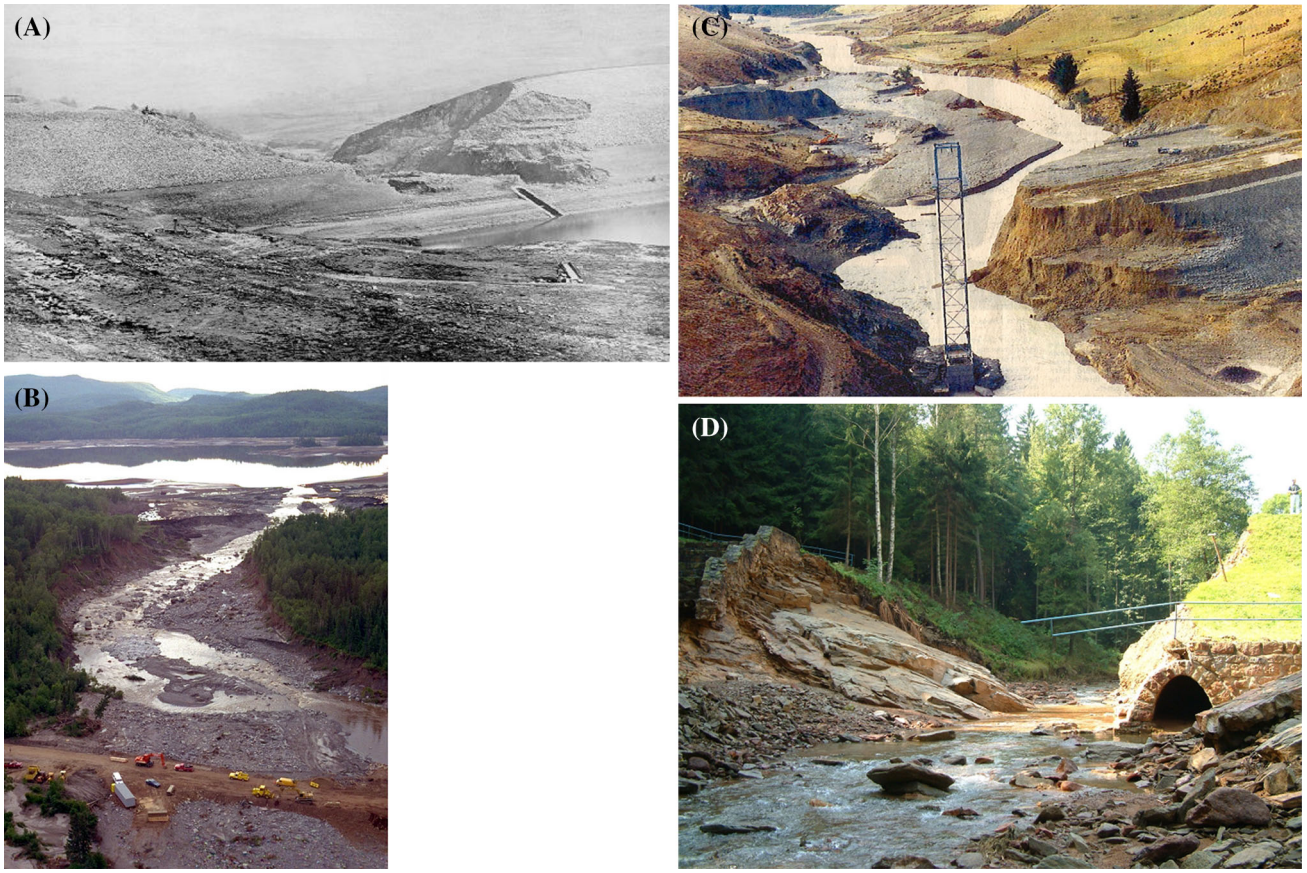

Fig. 3 Embankment dam failures. **a** The ruptured Dale Dyke dam embankment (UK) viewed from inside the reservoir, a few days after the disaster—completion: 1863, failure on 11 March 1864 because of piping and poor construction standards, 150 lives lost, **b** Lake Ha!Ha! failure (Canada) (Courtesy of Natural Resources Canada)—failure in July 1996 because of inadequate spillway capacity, **c** failed Opuha embankment dam (NZ) on 6 February 1997 (Courtesy of Tonkin and Taylor)—completion: 1999, $H = 50$ m, $L = 100$ m, failure by flood overtopping during construction, **d** failed Glasshütte embankment dam (Germany) looking upstream (Courtesy of Dr Antje Bornschein)—completion: 1953, $H = 9$ m, failure on 12 August 2002 because of inadequate spillway capacity

The overtopping of fluvial and coastal embankments was documented worldwide. During Hurricane Katrina in August 2005, several embankments protecting New Orleans and its surroundings were overtopped and breached, contributing to some extensive flooding [5]. Figure 2b illustrates the overtopping of an earthfill dyke along the Qiantang River estuary in August 2011. The flood tide combined with a powerful storm surge during Typhoon Nanmadol to cause an abnormally high tidal bore which overtopped the river dykes causing massive damages. Recent failures of coastal embankments were observed during the March 2011 Tohoku tsunami in Japan [39, 47]. Figure 2c shows a physical study of coastal barrier conducted in 2012 to develop safer tsunami protection structures. The movie 1 highlights the rushing motion of water past and impact onto the rubble mound structure ("Appendix", Table 1).

During the last five decades, a number of overtopping protection systems were developed for embankments. These include overtopping concrete protection systems, sheet-piles, gabions, reinforced earth, MEL spillways and embankment stepped spillway. In this contribution, several embankment overflow protection systems are presented and discussed, after a brief discussion of the embankment breaching process. The experience gained during the past decades is discussed.

2 Embankment breaching

The breaching of an overtopped embankment is a relatively slow process, for example, in comparison to the failure of a concrete dam. While the latter may be a sudden, explosive failure, an earthfill structure may sustain some overtopping for some times before the breach develops and progressively opens leading to the complete failure (Fig. 3). For example, the Glashütte dam (Fig. 3d) was overtopped for near 140 min before the wall failed within 30 min [7].

Table 1 Video movies of embankment overtopping

Video movie	Video name	Duration (s)	Description
Video No. 1	Movie1_IMGP0342.avi	7	Physical modelling of tsunami wave impacting onto and overtopping a coastal embankment barrier. Experiments conducted at Nihon University (Koriyama campus, Fukushima prefecture)
Video No. 2	Movie2_IMGP3427.avi	11	Breach development of a non-cohesive embankment ($H = 0.3$ m, $L = 1.5$ m, $d_{50} = 0.3$ mm) at the University of Auckland (NZ). Experiment conducted with constant upstream reservoir head

Figure 3 shows several examples of embankment dam failures, and Fig. 4 presents some photographs of the embankment breaching process.

Several studies on embankment breach were conducted during the last decade [6, 11, 18, 20, 30, 31, 38, 41, 46, 49]. Most physical studies under carefully controlled laboratory flow conditions, together with prototype observations, showed that the embankment breach starts with an initiation phase, followed by a rapid development of the breach, and then an enlargement of breach width once the breach invert reaches the channel bed rock. Observations of embankment breach scour showed a challenging similarity with the flow in a MEL weir inlet during the breach development [10, 34, 50]. This was nicely illustrated by two seminal physical studies of the breaching of non-cohesive embankment structures [18, 46]. It is also seen in Figs. 4b and 5a, and movie 2 ("Appendix", Table 1). Figure 4b shows the initial stages of the breach development (first 5 photographs), with some basic definitions in Fig. 5a, while the movie 2 shows the progressive enlargement of the breach during the development. Figure 5 presents some quantitative data by Coleman et al. [18].

A flow net analysis of the physical data of Coleman et al. [18] was conducted, and the three-dimensional flow cross-sectional areas were measured along equipotential planes at different times [10]. A typical example is shown in Fig. 5b in the form of the breach cross-sectional shapes below the waterline. The results indicated that the flow through the embankment breach was transcritical: that is, the flow was about critical between the inlet lip and the throat when the total head remained constant (Fig. 5c, d). Head losses occurred downstream of the throat when the flow streamlines diverged and flow separation occurred at the lateral boundaries. Typical results are shown in Fig. 5c, d where the dimensionless total head H/H_1 is plotted as a function of the dimensionless centreline location, where H_1 is the upstream total head above downstream channel elevation, and L is the embankment base length. Visually, the flow through the breach between the inlet lip to throat was somehow similar to the flow through a MEL spillway inlet (see next paragraph). For example, let us compare Fig. 4b with Fig. 6a.

The breach inlet length measured along the breach centreline between inlet lip and throat was about $L_{inlet}/B_{max} = 0.5$–0.6, where B_{max} is the free-surface width at the upper inlet lip (Fig. 5a). During the development of the breach, the outflow discharge equalled:

$$Q = C_D \times B_{max} \times \sqrt{g \times \left(\frac{2}{3} \times H_1\right)^3} \quad (1)$$

where C_D is a dimensionless discharge coefficient ($C_D \sim 0.6$). During an overtopping event, the breach size increases with time resulting in the hydrograph of the breach. In Eq. (1), both the breach free-surface width B_{max} and upstream total head H_1 are functions of time as well as embankment characteristics and reservoir size. For an infinitely long reservoir, a re-analysis of embankment breach data suggested that the inlet lip elevation z_{lip}, the inlet lip width B_{max} and the throat width B_{min} varied with time as:

$$\frac{z_{lip}}{H_1} = 1.08 \times \exp\left(-0.0013 \times t \times \sqrt{\frac{g}{H_1}}\right) \quad \text{for} \quad t \times \sqrt{\frac{g}{H_1}} < 1{,}750 \quad (2)$$

$$\frac{B_{max}}{H_1} = 2.73 \times 10^{-4} \times \left(t \times \sqrt{\frac{g}{H_1}}\right)^{1.4} \quad \text{for} \quad t \times \sqrt{\frac{g}{H_1}} < 1{,}000 \quad (3)$$

$$\frac{B_{min}}{H_1} = 4.01 \times 10^{-7} \times \left(t \times \sqrt{\frac{g}{H_1}}\right)^{2.3} \quad \text{for} \quad t \times \sqrt{\frac{g}{d_o}} < 1{,}000 \quad (4)$$

where g is the gravity acceleration, H_1 is the upstream total head, z_{lip} is the inlet lip elevation on the breach centreline and B_{min} is the free-surface width at the breach throat [10]. Equations (2), (3) and (4) were derived for cohesionless materials and valid only during the breach development.

Fig. 4 Embankment breaching. **a** Marmot Dam cofferdam breaching (USA) on 19 October 2007 (Courtesy of Portland General Electric)—the cofferdam was built as part of the Marmot (concrete) dam removal to restore fish migration along the Sandy River, **b** physical modelling of non-cohesive embankment dam failure at the University of Auckland in 2012—$H = 0.3$ m, $L = 1.5$ m, $d_{50} = 0.3$ mm, constant upstream head experiment—flow direction from *left to right* with the reservoir on the *right*—the first five shots (*1–5*) were taken during the breach development; the last two shots (*7–8*) show details of the breach after the reservoir draining

3 Embankment overtopping protection systems (1) the minimum energy loss (MEL) inlet design

3.1 Presentation

An unusual embankment overflow protection system is the MEL inlet design introduced in Australia during the 1970s [35, 36]. The first MEL inlet structure was the Redcliffe storm waterway system (1960); the inlet system is still in use and passed floods greater than its design flow ($Q_{des} = 25.8$ m^3/s) without damage [13, 34]. The MEL inlet was developed to pass large floods with MEL and afflux, where the afflux is the rise in upstream water level caused by the presence of the embankment structure. Commonly used in culvert design, the afflux is a quantitative measure of the upstream flooding caused by the hydraulic structure. In the approach flow region, the water discharge is smoothly converged towards a streamlined chute, the MEL inlet system, and the design yields a nearly constant total head along the waterway (Fig. 6). Figure 6 presents two prototype applications during a low flow operation. The approach flow region and MEL waterway are streamlined to avoid significant form losses. At design conditions, the flow may be critical from the inlet lip to the chute toe. The MEL inlet system was developed for embankment dam applications where the river catchment is characterised by large rainfalls and a very small bed slope. Figure 6a shows the MEL inlet at Lake Kurwongbah dam spillway: the efficient inlet design allowed and extra 0.457 m of water storage for the same maximum discharge capacity [35]. Figure 6b presents an overflow MEL embankment weir.

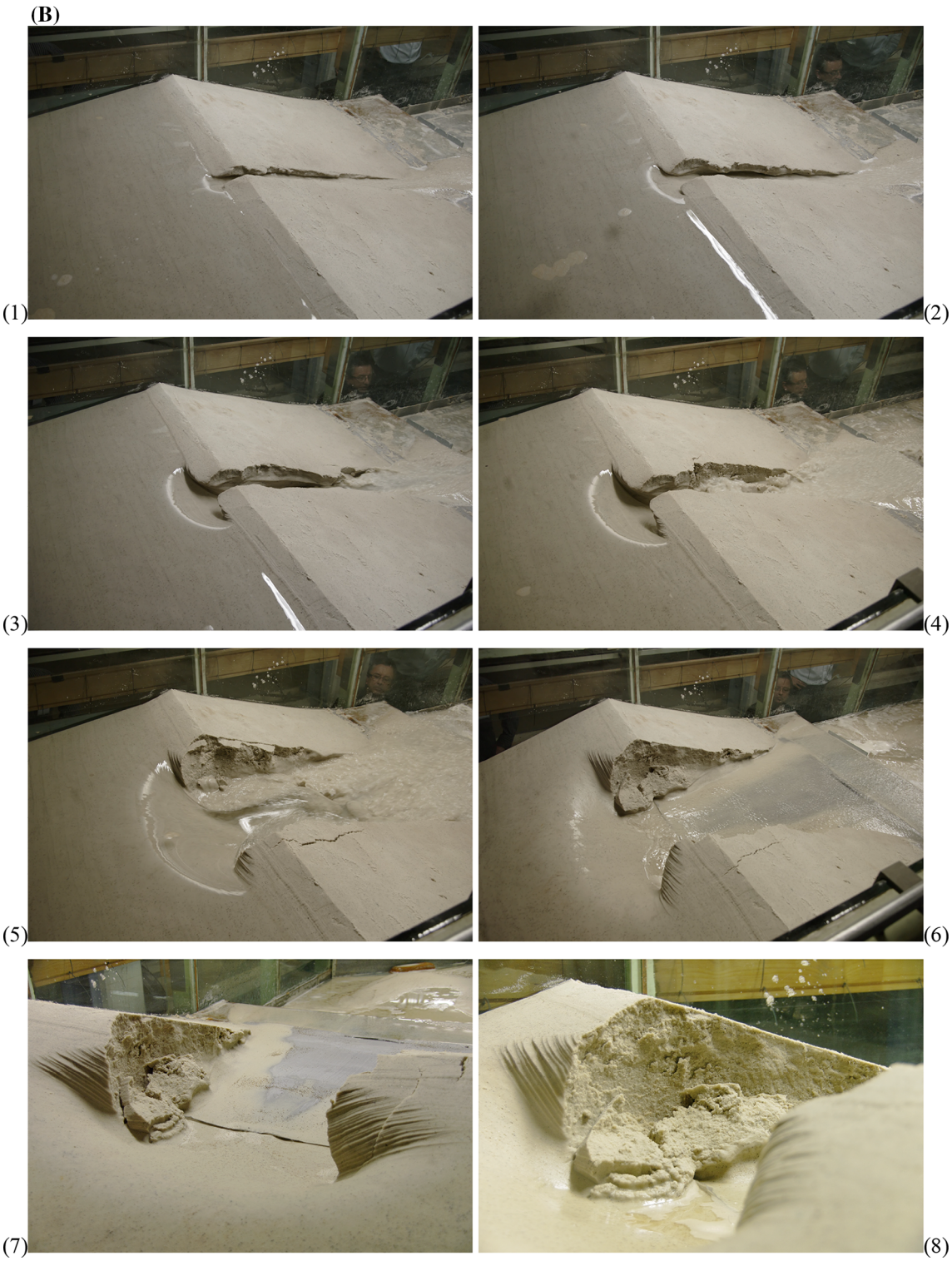

Fig. 4 continued

A MEL inlet is a streamlined channel with converging chute sidewalls, and the spillway chute is relatively flat. A downstream energy dissipator is concentrated near the channel centreline at the downstream end. At the chute toe, the inflow Froude number remains low and the rate of energy dissipation is small compared to a traditional weir. As an example, the Chinchilla MEL weir was designed to give zero afflux at design flow (Q_{des} 850 m^3/s); in 1974, the

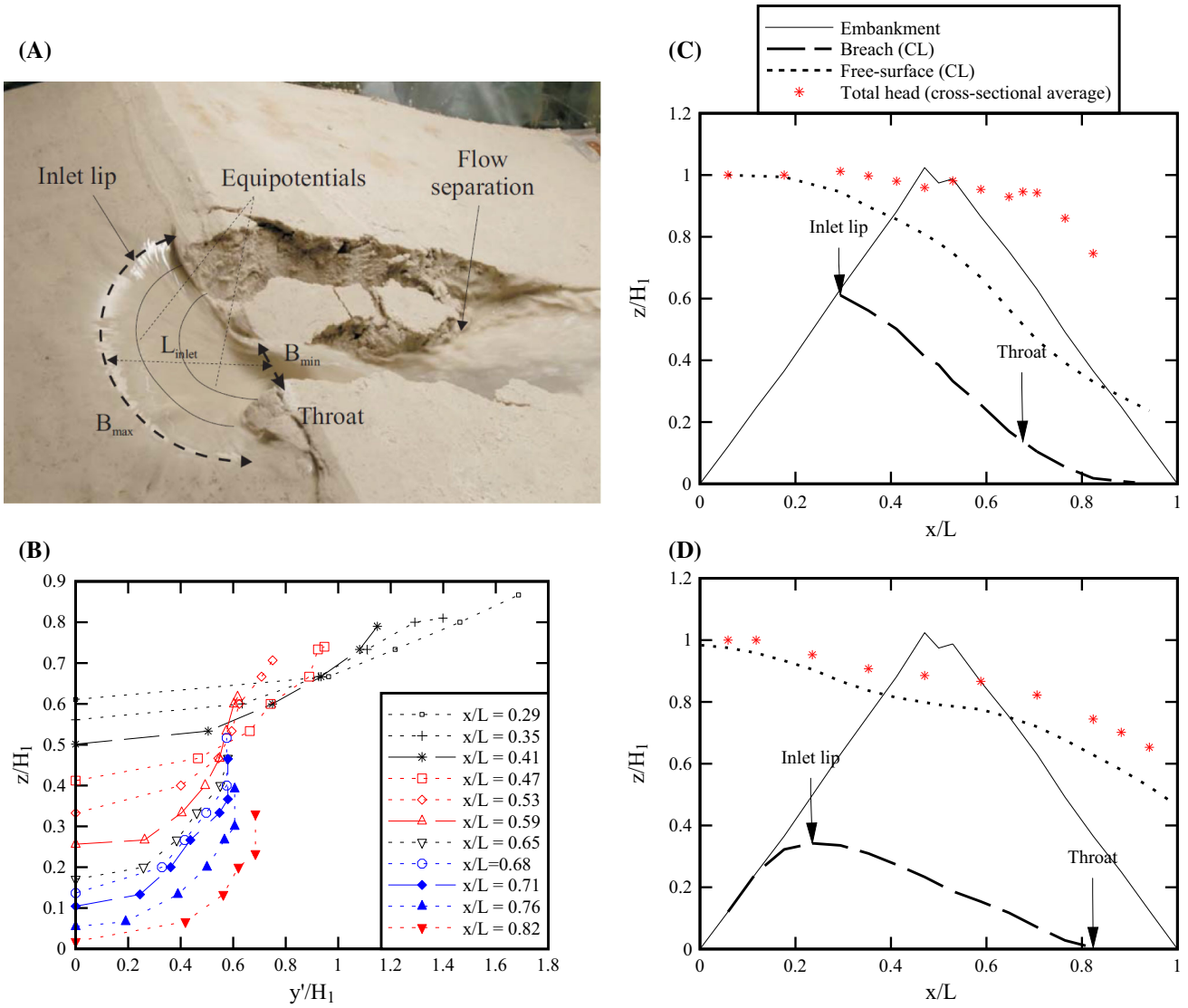

Fig. 5 Physical measurements of non-cohesive embankment breaching—data set: Coleman et al. [18], data re-analysis by the author, embankment height; $H_1 = 0.30$ mm, length: $L = 1.7$ m, upstream and downstream slopes: 1V:2.7H, 1.6 mm sand, constant upstream head experiment. **a** Definition sketch, **b** breach cross-sectional shape along equipotentials below the waterline, $t = 87$ s, $Q_{breach} = 0.024$ m^3/s, **c** longitudinal bed elevation and total head along breach centreline, $t = 87$ s, $Q_{breach} = 0.024$ m^3/s, **d** longitudinal bed elevation and total head along breach centreline, $t = 147$ s, $Q_{breach} = 0.071$ m^3/s

overflow discharge was estimated at 1,130 m^3/s and the measured afflux was <100 mm [48].

3.2 Design considerations

The purpose of a MEL inlet is to minimise afflux and energy dissipation at the design discharge, while avoiding scour and bank erosion at the toe of the chute. The inlet is curved in plan to converge the chute flow, and the chute slope is relatively flat. Assuming a relatively broad crest and a smooth approach without head loss, the discharge capacity of the MEL inlet equals:

$$Q = B_{max} \times \sqrt{g} \times \left(\frac{2}{3} \times (H_1 - z_{crest})\right)^{3/2} \quad (5)$$

where $H_1 - z_{crest}$ is the upstream head above spillway crest and B_{max} is the crest width (see definition in Fig. 5a). A MEL spillway channel could be designed to achieve critical flow conditions at any position along the chute and, hence, to prevent the occurrence of a downstream hydraulic jump with high tailwater conditions. Assuming negligible energy loss along the inlet, the channel width B at any elevation $z - z_{crest}$ beneath the crest above the weir toe should satisfy:

Fig. 6 Minimum energy loss (MEL) spillway and weir. **a** Minimum energy loss spillway inlet of Lake Kurwongbah (Brisbane, Australia) in operation on 29 January 2013, **b** lemontree minimum energy weir (Australia) on 8 November 1997 for a small discharge ($Q \ll Q_{des}$)

$$B = B_{max} \times \left(\frac{H_{des} - z_{crest}}{H_{des} - z}\right)^{3/2} \quad \text{Ideal conditions} \qquad (6)$$

where H_{des} is the design upstream head. Equation (6) is only valid at design flow conditions. In practice, the variations of the tailwater elevations with discharge are important and a weak jump takes place at the inlet toe as seen in Fig. 6b. The downstream conjugate depth is fixed by the tailwater conditions downstream of the hydraulic jump.

3.3 Prototype experiences

The MEL spillway structures were designed with the concept of constant total head, hence zero afflux, associated with some physical modelling. Indeed, the above predesign calculations are typically validated with 1:50–1:80 undistorted scale models with fixed bed.

The MEL overflow spillways are typically earthfill structures protected by concrete slabs (Fig. 6), and the construction costs must be minimum. The operations of a number of MEL spillways and weirs were documented, with a complement of field inspections and discussions with designers (Table 2) [9, 14]. A number of MEL structures were observed to operate at design flow conditions and for floods larger than design. Inspections during and after flood events showed the sound operation together with little maintenance. The successful operation of several structures for over 40 years has highlighted further considerations. Some improper approach flow conditions could affect adversely the spillway operation. MEL weirs are typically earthfill structures, and the spillway section is protected by concrete slabs. An efficient drainage system must be installed underneath the chute slabs. A known issue is the overtopping risk during construction as for the Sandy Creek weir and Chinchilla weir (twice).

Table 2 Characteristics of minimum energy loss weirs and spillway inlets in Australia (All MEL structures are still in use)

Minimum energy loss inlet structure (1)	Date (2)	Q_{des} m^3/s (3)	H_{dam} m (4)	B_{max} m (5)	B_{min} m (6)
MEL overflow weirs					
Redcliffe Qld	1959	25.8	1.2	19.5	5.5
Sandy Creek weir, Clermont Qld	1962–1963	849.5	6.1	115.8	<53 m
Chinchilla weir, Chinchilla Qld	1978	850.0	14.0	410.0	–
Lemontree weir, Milmerran Qld	1980s	–	4.0	–	–
MEL spillway inlets					
Lake Kurwongbah, Petrie Qld	1958–1969	849.5	25.0	106.7	30.5
Swanbank Power House, Ipswich Qld	1965	160.0	~6–8	45.7	7.31

Q_{des}, design discharge; B_{max}, inlet lip (crest) width; B_{min}, chute toe width; H_{dam}, dam height above foundation

4 Embankment overtopping protection systems (2) the gabion stepped weir

4.1 Presentation

A gabion is a basket filled with earth or stone for use in fortification and engineering. Gabions are extensively used for earth retaining structures as well as hydraulic structures. As a construction material, the advantages are their stability, low cost, flexibility and porosity. The gabion porosity is important to prevent the build-up of uplift pressures. Figure 7 shows an overflow gabion structure.

Modern box gabions consist of rockfill material enlaced by a basket or a mesh, shaped like a rectangular box. Typical gabion dimensions are heights of 0.5–1 m, a width equal to the height and length-to-height ratio between 1.5 and 4. Long gabions may be subdivided into cells by inserting diaphragms made of mesh panels to strengthen the gabion.

Fig. 7 Gabion weir: Robina stepped weir No. 1 (Gold Coast, Australia) on 2 April 1997, shortly after completion: $h \sim 0.5$ m, $h/l \sim 0.5$

The wire is normally made of soft steel with a zinc coating. In practice, the durability of gabion structures relies strongly upon the quality of the mesh and wires. The gabion filling consists of loose or compacted rocks. The stone size must equal at least 1–1.5 times the mesh size but should not be larger than 2/3 of the minimum dimension of the gabion. The use of small-sized stone, typically 1.5 times the mesh size, permits a better adaptability of the gabion boxes to deformation.

4.2 Gabion stepped weir design

The dimensions of the gabion and the design discharge are the two basic design parameters controlling the hydraulic operation of the chute. The step height h is typically the gabion height, although h might equal twice or three times the gabion height in some cases. The stepped chute slope ranges from 1V:4H to 1V:2H. For a gabion structure only, the choice of a steep slope with a skimming flow regime may reduce the number of gabions and the overall structure cost. For an embankment with gabion overtopping, a flat slope may be more appropriate for the stability requirements of the earthfill structure. The design considerations for the stability of gabion weirs are generally the same as for any gravity structure. The calculations of structural stability involve checking the stability of the weir against overturning, sliding and uplift. Inclined (upward) gabion stepped spillways may also be used [42]. Larger energy dissipation is achieved, but their construction requires greater care.

In comparison with concrete spillways, the flow above a stepped gabion chute is characterised by (1) some interactions between the surface overflow and seepage flow and (2) the rougher surface of the gabion steps [51]. The hydraulics might be further complicated by the presence of timber or concrete lining [33]. The seepage will modify spatially the surface discharge. Some associated issues were discussed by Curtis and Lawson [19] and Kells [32].

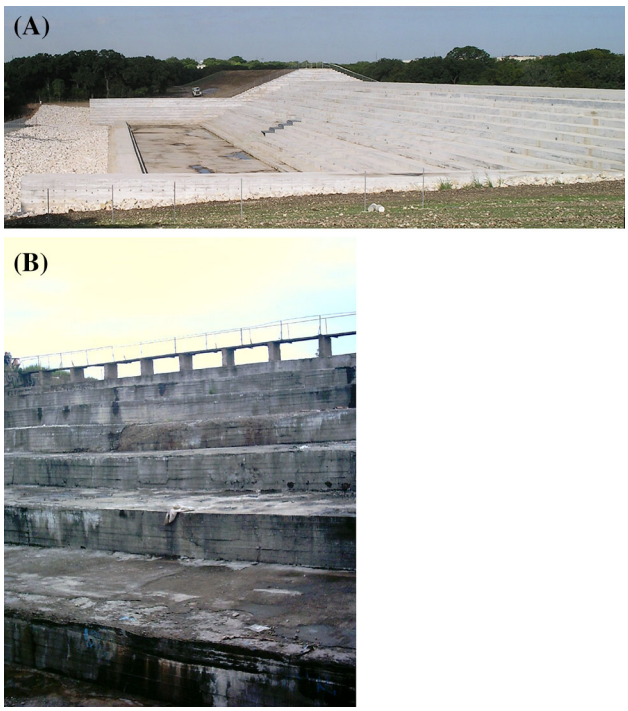

Fig. 8 Concrete stepped chutes above embankments. **a** Salado Creek Dam Site 15R in February 2005 (Courtesy of Craig Savela, USDA), **b** old seventeenth-century rockfill embankment with timber crib overflow near Moscow (Russia) (Courtesy of Dr Marat Mirzoev)—a concrete stepped chute was installed in the last 20 years

4.3 Discussion

The performances of gabion stepped weirs are often restricted by the gabion resistance to damage and their stability. Sediments and debris carried by the stream flow may affect and fracture the gabion mesh. With large-size debris, it is common practice to protect the step surfaces with timber, steel sheets, concrete facing or even reinforced concrete slab [1, 43]. Figure 8b shows a more extreme example of concrete facing.

5 Embankment overtopping protection systems (3) the concrete stepped spillway

5.1 Presentation

During the last decades, a number of embankment dams were equipped with an overflow concrete stepped spillway [8] (Fig. 8). Applications included both primary and secondary spillway structures: Fig. 8a illustrates a recent embankment dam equipped with a primary embankment

overflow stepped spillway. Most modern stepped spillways consist of flat horizontal steps, although different step configurations may be considered [3, 23, 27, 29]. The preferred construction method is the placement of roller compacted concrete (RCC) overlays on the downstream embankment slope [21]. RCC is defined as a no-slump consistency concrete that is placed in horizontal lifts and compacted by vibratory rollers. During the construction, the RCC is placed typically in a succession of 0.2–0.4 m thick overlays with a width >2.5 m for proper hauling, spreading and compacting. The advantages of RCC construction are the cost-effectiveness and the short duration of construction. For an embankment overtopping protection, exposed RCC is frequently used for secondary spillways with infrequent overflows. In harsh climatic conditions, or for a primary spillway, a conventional concrete protection layer may be installed to protect the RCC. In all the cases, a drainage layer beneath the concrete overlays is essential to prevent uplift pressures. Its purpose is to relieve pore pressure at the interface between the embankment and concrete stepped spillway. The drainage layer may be complemented by a series drain holes formed through the RCC during placement. At the downstream end of the overflow, a cut-off wall must be built to prevent the undermining of the concrete system during discharge.

5.2 Hydraulic considerations

An embankment stepped spillway is typically designed to operate in a skimming flow regime [8]. As part of pre-design calculations, the constraints are the embankment height, embankment downstream slope and design discharge. The variable parameters include the type of crest shape, the chute width and possibly the step height. Yet, the step height h is always selected as a multiple of the RCC overlay height, yielding step heights $h = 0.2$–0.9 m [25].

In a skimming flow above the stepped spillway, the upstream flow is characterised by a developing boundary layer [2, 37] (Fig. 9). When the outer edge of the boundary layer interacts with the free surface, the turbulent shear stress becomes greater than the surface tension force per unit area resisting the interfacial breakup and free-surface aeration takes place [15, 22]. The location and flow depth at the inception point of free-surface aeration may be estimated as:

$$\frac{L_I}{h \times \cos\theta} = 9.72 \times (\sin\theta)^{0.080} \times \left(\frac{q}{\sqrt{g \times \sin\theta \times (h \times \cos\theta)^3}}\right)^{0.71} \quad (7)$$

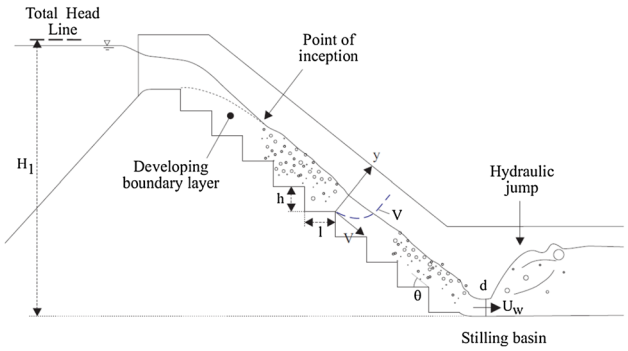

Fig. 9 Sketch of an embankment overtopping stepped spillway

$$\frac{d_I}{h \times \cos\theta} = \frac{0.403}{(\sin\theta)^{0.04}} \times \left(\frac{q}{\sqrt{g \times \sin\theta \times (h \times \cos\theta)^3}}\right)^{0.59} \quad (8)$$

where q is the discharge per unit width ($q = Q/B$), L_I the longitudinal distance from the chute crest to the apparition of white waters at the free-surface, d_I the flow depth at the inception point, g the gravity acceleration and θ the angle between the pseudo-bottom formed by the step edges and the horizontal.

If the channel is long enough for the flow to reach uniform equilibrium, the characteristic flow depth d equals:

$$d = \sqrt[3]{\frac{f_e \times q^2}{8 \times g \times \sin\theta}} \quad (9)$$

where f_e is the Darcy friction factor estimated based upon experimental air–water flow friction factor data [12, 17]. If the flow does not reach normal flow conditions before the downstream end of the spillway, the flow is gradually varied downstream of the inception point of air entrainment. Combining some well-documented experimental results together with theoretical calculations, an empirical correlation was derived in terms of the downstream spillway velocity as a function of the upstream above crest and discharge [24]:

$$\frac{U_w}{V_{\max}} = 0.00105 \times \left(\frac{H_1}{\sqrt[3]{q^2/g}}\right)^2 - 0.0634 \times \left(\frac{H_1}{\sqrt[3]{q^2/g}}\right) + 1.202 \quad (10)$$

where H_1 is the upstream total head above chute toe, d_c is the critical depth, $V_{\max}$ is the ideal flow velocity deduced from the Bernoulli principle and U_w is the downstream velocity. Such an approach may be used for pre-design calculations assuming a friction coefficient $f_e = 0.2$, and it

was only validated for moderate stepped spillway slopes ($15° < \theta < 25°$). These preliminary estimates must be checked with some solid physical modelling, based upon undistorted scale models with scaling ratios no greater than 3:1.

For short stepped chutes and large discharges, the flow may not be fully developed before the downstream of the chute. That is, the chute length may be smaller than the distance between crest and inception point of free-surface aeration. A simple method was developed to predict the depth-averaged flow properties [8, 37].

6 Embankment overtopping protection systems (4) the precast concrete block spillway

A related form of stepped overflow protection system is the precast concrete block spillway developed in Russia [28, 44]. The spillway is made of individual blocks placed in an overlapping staircase fashion, and the stepped design contributes to the energy dissipation (Fig. 10). Figure 10a shows a structure in which the precast concrete block spillway is the primary flood release structure. Figure 10b illustrates an older embankment structure refurbished with a new spillway on the downstream embankment slope. An interesting feature is the flexibility of the channel bed allowing differential settlements of the earthfill embankment, while another feature is the fairly short construction time on site.

The Russian engineers developed a strong expertise in the design of concrete wedge blocks. This was supported by extensive testing. For large discharges, each block should be tied to adjacent blocks, possibly made of reinforced concrete. A step height-to-length ratio in the range 1:4–1:6 may ensure maximum stability of the blocks during the overtopping. Drains must be placed in areas of sub-

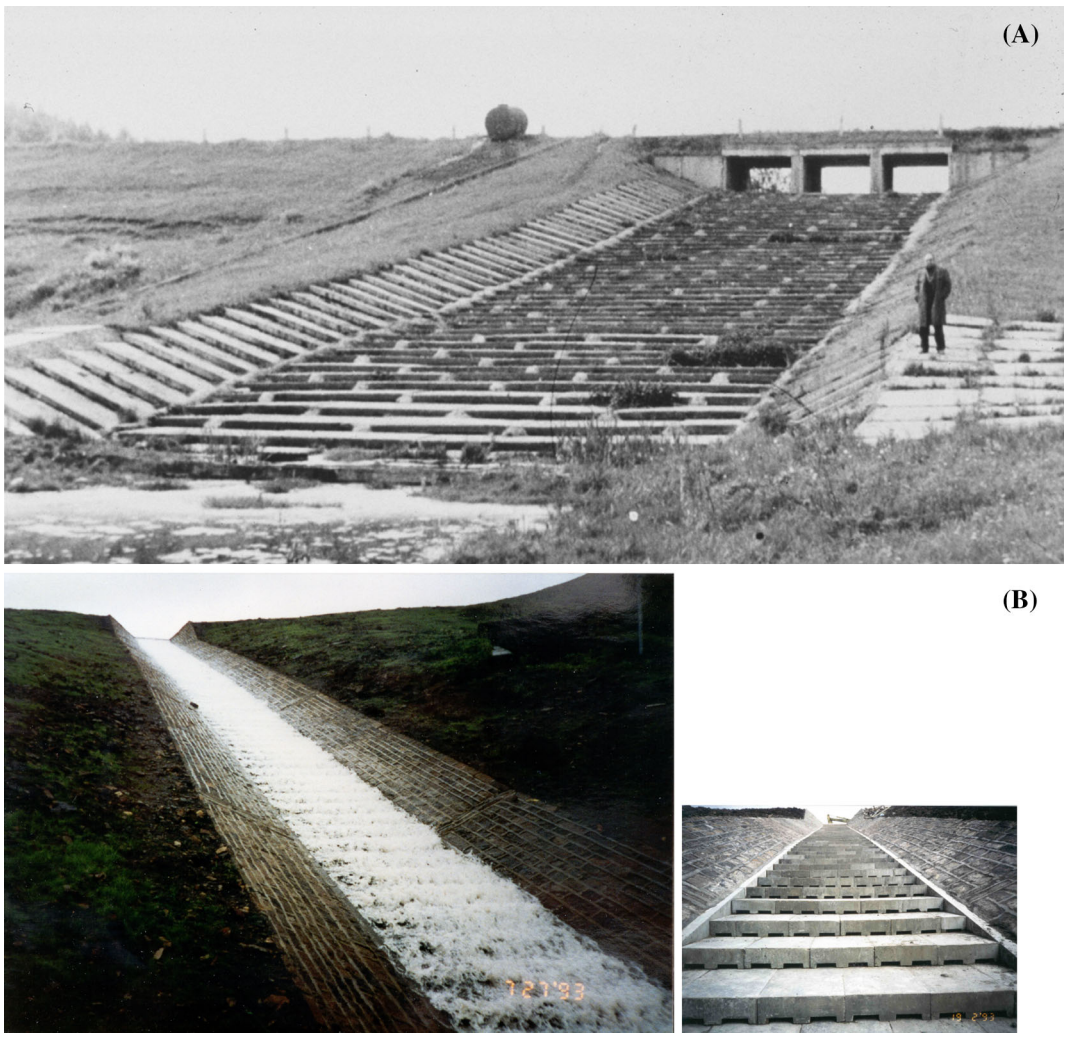

Fig. 10 Embankment dams with precast concrete block spillway. **a** Sosnovsky dam (Russia) (Courtesy of Prof. Y. Pravdivets), **b** Brushes Clough dam (UK) in 1993 (Courtesy of Mr Gardiner, NWW)—*left* small overflow; *right* details of the concrete block placement

atmospheric pressure to relieve uplift pressures (Fig. 10b). Figure 10b illustrates some drains on the vertical step face.

7 Basic design considerations

For an embankment structure, the uppermost important criterion is the stability of the earthfill embankment material. The construction must be of good quality and the design simple and sound. Seepage may occur in saturated embankment, and the resulting uplift pressures might damage or destroy the stepped channel and the whole structure. An adequate drainage is essential. A filter and erosion protection layer is typically laid on the downstream embankment slope (e.g. geotextile membrane) before placing the overflow protection. The layer has the functions to filter the seepage flow out of the subsoil and to protect the subsoil layer from erosion by flow in the drainage layer.

The hydraulic design of the spillway is critical. Key issues include (a) the maximum discharge capacity estimate, (b) the downstream dissipation structure and (c) the high level of hydraulic expertise required. First, the spillway capacity must be adequately estimated to prevent any overflow over the unprotected embankment. At the downstream end of the spillway, the turbulent kinetic energy of the flow must be dissipated safely. Common dissipation designs include the hydraulic jump stilling basin (Fig. 9) and a flip bucket to deflect the water away from the chute toe. Altogether, the experience has shown that the hydraulic design of embankment overflow systems requires a high level of expertise.

Practically, some basic down-to-earth considerations must be taken into account. There were accounts of vandalism in a few projects, including motor bikes riding up and down the Brushes Clough dam spillway (Fig. 10b) and damaging the precast concrete blocks, and locals stealing mesh of gabion structures to build local fences. Alternative embankment overtopping protection systems include timber cribs, sheet-piles, riprap and gabions and reinforced earth [8, 14].

7.1 Hydraulics considerations

During the last three decades, a number of embankment dam spillways were built with a range of construction techniques. The most common is the stepped profile designed to increase the rate of energy dissipation on the spillway chute [8, 40]. However, the design engineers must assess accurately the turbulent kinetic energy dissipation above the steps, in particular for large discharges per unit width corresponding to the skimming flow regime. A characteristic feature of skimming flows is the high level of turbulence and free-surface aeration [43, 45]. The water flows down the steps as a coherent free-stream skimming over the pseudo-bottom formed by the step edges. In the step cavities, the turbulent recirculation is maintained through the transmission of shear stress from the free stream. At the free-surface, air is continuously trapped and released, and the resulting two-phase mixture interacts with the flow turbulence yielding some intricate air–water structure associated with complicated energy dissipation mechanisms [16, 26].

8 Conclusion

In recent years, a number of embankment overtopping protection systems were developed for coastal barriers, earthfill dams and river dykes. The overtopping protection systems include concrete stepped overtopping protection, MEL spillway, gabion stepped spillways and precast concrete block protection systems. For embankments higher than 5–10 m, the concrete stepped spillway is a sound design technique well suited to small to large discharges. The flow down the stepped cascade is characterised by some strong aeration, high turbulence of the flow and a significant rate of energy dissipation.

A number of embankment protection systems have been in operation for three to four decades. The prototype experience provides valuable informations. Based upon past accident and failure forensic investigations, it is clearly understood that a safe operation relies upon a sound design and a good quality of construction, suitable flow conditions, together with regular maintenance. Ultimately, there is no better proof of design soundness than successful prototype operation.

It is acknowledged that there are some differences between the various applications, for example, with regard to the breaching process and optimum protection systems linked to different boundary conditions. The present contribution focused mostly on the hydraulic engineering, although both hydraulic and geotechnical expertise is required for any earthfill embankment project.

Acknowledgments The author thanks all the individuals and organisations who provide him with relevant informations, including Professor Colin Apelt. The author acknowledges some helpful discussion with the associate editors. The financial support of the Australian Research Council is acknowledged (Grants ARC DP0878922 & DP120100481).

References

1. Agostini R, Bizzarri A, Masetti M, Papetti A (1987) Flexible gabion and Reno mattress structures in river and stream training works. Section one: Weirs, 2nd edn. Officine Maccaferri, Bologna

2. Amador A, Sanchez-Juny M, Dolz J (2006) Characterization of the nonaerated flow region in a stepped spillway by PIV. J Fluids Eng ASME 128(6):1266–1273
3. Andre S, Boillat JL, Schleiss AJ, Matos J (2004) Energy dissipation and hydrodynamic forces of aerated flow over macro-roughness linings for overtopped embankment dams. In: Proceedings of the international conference on hydraulics of dams and river structures, Tehran, Iran, Balkema Publ., The Netherlands, pp 189–196
4. ASCE (1994) Alternatives for overtopping protection of dams. ASCE, New York, USA, Task Committee on Overtopping Protection
5. ASCE (2007) The New Orleans hurricane protection system: what went wrong and why. American Society of Civil Engineers, Hurricane Katrina External Review Panel, Reston VA, USA
6. ASCE/EWRI Task Committee on Dam/Levee Breaching (2011) Earthen embankment breaching. J Hydraul Eng ASCE 137(12):1549–1564. doi:10.1061/(ASCE)HY.1943-7900.0000498
7. Bornschein A, Pohl R (2003) Dam break during the flood in Saxony/Germany in August 2002. In: Ganoulis J, Prinos P (eds) Proceedings of the 30th IAHR Biennial Congress, Thessaloniki, Greece, vol C2, pp 229–236
8. Chanson H (2001) The hydraulics of stepped chutes and spillways. Balkema, Lisse, The Netherland
9. Chanson H (2003) Minimum energy loss structures in Australia: historical development and experience. In: Sheridan N (ed) Proceedings of the 12th national engineering heritage conference. Institution of Engineers, Australia, Toowoomba Qld, Australia, pp 22–28
10. Chanson H (2004) Overtopping breaching of noncohesive homogeneous embankments. J Hydraul Eng ASCE 130(4):371–374
11. Chanson H (2005) The 1786 earthquake-triggered landslide dam and subsequent dam-break flood on the Dadu river, southwestern China. Geomorphology 71:437–440. doi:10.1016/j.geomorph.2005.04.017
12. Chanson H (2006) Hydraulics of skimming flows on stepped chutes: the effects of inflow conditions? J Hydraul Res IAHR 44(1):51–60
13. Chanson H (2007) Hydraulic performances of minimum energy loss culverts in Australia. J Perform Constr Facil ASCE 21(4):264–272. doi:10.1061/(ASCE)0887-3828(2007)21:4(264)
14. Chanson H (2009) Embankment overtopping protections system and earth dam spillways. In: Hayes WP, Barnes MC (eds) Dams: impact, stability and design. Nova Science Publishers, Hauppauge NY, USA, Chapter 4, pp 101–132
15. Chanson H (2009) Turbulent air–water flows in hydraulic structures: dynamic similarity and scale effects. Environ Fluid Mech 9(2):125–142. doi:10.1007/s10652-008-9078-3
16. Chanson H, Toombes L (2002) Experimental investigations of air entrainment in transition and skimming flows down a stepped chute. Can J Civ Eng 29(1):145–156
17. Chanson H, Yasuda Y, Ohtsu I (2002) Flow resistance in skimming flows and its modelling. Can J Civ Eng 29(6):809–819
18. Coleman SE, Andrews DP, Webby MG (2002) Overtopping breaching of noncohesive homogeneous embankments. J Hydraul Eng ASCE 128(9):829–838
19. Curtis RP, Lawson JD (1967) Flow over and through rockfill banks. J Hydraul Div ASCE 93(HY5):1–21
20. Dai FC, Lee CF, Deng JH, Tham LG (2005) The 1786 earthquake-triggered landslide dam and subsequent dam-break flood on the Dadu river, southwestern China. Geomorphology 65:205–221
21. Ditchey EJ, Campbell DB (2000) Roller compacted concrete and stepped spillways. In: Minor HE, Hager WH (eds) Proceedings of the international workshop on hydraulics of stepped spillways, Zürich, Switzerland, Balkema Publ., pp 171–178
22. Ervine DA, Falvey HT (1987) Behaviour of turbulent water jets in the atmosphere and in plunge pools. In: Proceedings of the institution of civil engineers, London, Part 2, March 1987, vol 83, pp 295–314
23. Felder S, Chanson H (2014) Effects of step pool porosity upon flow aeration and energy dissipation on pooled stepped spillways. J Hydraul Eng ASCE 140(4), Paper 04014002. doi:10.1061/(ASCE)HY.1943-7900.0000858
24. Gonzalez CA (2005) An experimental study of free-surface aeration on embankment stepped chutes. Ph.D. thesis, Department of Civil Engineering, The University of Queensland, Brisbane, Australia
25. Gonzalez CA, Chanson H (2007) Hydraulic design of stepped spillways and downstream energy dissipators for embankment dams. Dam Eng 17(4):223–244
26. Gonzalez CA, Chanson H (2008) Turbulence and cavity recirculation in air–water skimming flows on a stepped spillway. J Hydraul Res IAHR 46(1):65–72
27. Gonzalez CA, Takahashi M, Chanson H (2008) An experimental study of effects of step roughness in skimming flows on stepped chutes. J Hydraul Res IAHR 46(1):24–35
28. Gordienko PI (1978) Reinforced-concrete-earth overflow dams. Dams & Spillways, Collection of works no. 61, Issue 2, MISI, Moscow, pp 3–17 (in Russian)
29. Guenther P, Felder S, Chanson H (2013) Flow aeration, cavity processes and energy dissipation on flat and pooled stepped spillways for embankments. Environ Fluid Mech 13(5):503–525. doi:10.1007/s10652-013-9277-4
30. Hanson GJ, Cook KR, Hunt SL (2005) Physical modeling of overtopping erosion and breach formation of cohesive embankments. Trans ASABE 48(5):1783–1794
31. Hunt SL, Hanson GJ, Cook KR, Kadavy KC (2005) Breach widening observations from earthen embankment tests. Trans ASAE 48(3):1115–1120
32. Kells JA (1993) Spatially varied flow over rockfill embankments. Can J Civ Eng 20:820–827
33. Kells JA (1995) Comparison of energy dissipation between nappe and skimming flow regimes on stepped chutes-discussion. J Hydraul Res IAHR 33(1):128–133
34. McKay GR (1970) Pavement drainage. In: Proceedings of the 5th Australian road research board conference, vol 5, Part 4, pp 305–326
35. McKay GR (1971) Design of minimum energy culverts. Research Report, Department of Civil Engineering, University of Queensland, Brisbane, Australia, 7 plates
36. McKay GR (1978) Design principles of minimum energy waterways. In: Porter KF (ed) Proceedings of the workshop on minimum energy design of culvert and bridge waterways, Australian Road Research Board, Melbourne, Australia, Session 1, pp 1–39
37. Meireles I, Matos J (2009) Skimming flow in the nonaerated region of stepped spillways over embankment dams. J Hydraul Eng ASCE 135(8):685–689
38. Morris MW, Hassan M, Vaskin KA (2007) Breach formation: field test and laboratory experiments. J Hydraulic Res 45(Special Issue):9–17
39. Ogasawara T, Matsubayashi Y, Sakai Y (2012) Characteristics of the 2011 Tohoku earthquake and tsunami and its impact on the northern Iwate coast. Coastal Eng J 54(1) Paper 1250003. doi:10.1142/S0578563412500039
40. Ohtsu I, Yasuda Y, Takahashi M (2004) Flow characteristics of skimming flows in stepped channels. J Hydraul Eng ASCE 130(9):860–869

41. Orendorff B, Rennie CD, Nistor J (2011) Using PTV through an embankment breach channel. J Hydro-Environ Res 5(4), Special Issue SI, pp 277–287. doi:10.1016/j.jher.2010.12.003
42. Peyras L, Royet P, Degoutte G (1991) Ecoulement et dissipation sur les déversoirs en gradins de gabions. J Houill Blanch 1:37–47
43. Peyras L, Royet P, Degoutte G (1992) Flow and energy dissipation over stepped gabion weirs. J Hydraul Eng ASCE 118(5):707–717
44. Pravdivets YP, Bramley ME (1989) Stepped protection blocks for dam spillways. Int Water Power Dam Constr 41(7):49–56
45. Rajaratnam N (1990) Skimming flow in stepped spillways. J Hydraul Eng ASCE 116(4):587–591
46. Rozov AL (2003) Modeling a washout of dams. J Hydraul Res IAHR 41(6):565–577
47. Suppasri A, Koshimura K, Imai K, Mas E, Gokon H, Muhari A, Imamura F (2012) Damage characteristics and field survey of the 2011 Great East Japan Tsunami in Miyagi Prefecture. Coastal Eng J 54(1), Paper 1250005. doi:10.1142/S0578563412500052
48. Turnbull JD, McKay GR (1974) The design and construction of Chinchilla weir—Condamine River Queensland. In: Proceedings of the 5th Australasian conference on hydraulics and fluid mechanics, Christchurch, New Zealand, vol II, pp 1–8
49. Vaskinn KA, Lovoll A, Hoeg K, Morris M, Hanson G (2004) Physical modeling of breach formation: large scale field tests. In: Proceedings of the Dam safety 2004, Association of State Dam Safety Officials, Phoenix Ariz, 16 p
50. Visser PJ, Vrijling JK, Verhagen HJ (1990) A field experiment on breach growth in sand-dykes. In: Edge B (ed) Proceedings of the 22nd international conference on coastal engineering, Delft, Netherlands, vol 2, pp 2097–2100
51. Wüthrich D, Chanson H (2014) Hydraulics, air entrainment and energy dissipation on gabion stepped weir. J Hydraul Eng ASCE 140(9):1–10. doi:10.1061/(ASCE)HY.1943-7900.0000919
52. Yin Y, Wang F, Sun P (2009) Landslide hazards triggered by the 2008 Wenchuan earthquake, Sichuan, China. Landslides 6(2):139–152